Prev. Nutr. Food Sci. 2022;27(4):448-456
https://doi.org/10.3746/pnf.2022.27.4.448
ISSN 2287-8602

Evaluation and Comparison of the Antimelanogenic Properties of Different Solvent Fractionated *Cnidium japonicum* Extracts in B16F10 Murine Melanoma Cells

Hyun Jin Jo[1], Jung Hwan Oh[2,3], Fatih Karadeniz[2], Youngwan Seo[4], and Chang-Suk Kong[1,2]

[1]Department of Food and Nutrition, College of Medical and Life Sciences, [2]Marine Biotechnology Center for Pharmaceuticals and Foods, and [3]Nutritional Education, Graduate School of Education, Silla University, Busan 46958, Korea
[4]Division of Convergence on Marine Science, College of Ocean Science and Technology, Korea Maritime and Ocean University, Busan 49112, Korea

ABSTRACT: *Cnidium japonicum* is a biennial halophyte found in the salt marshes and shores of Korea and widely used in traditional Korean medicine as an ingredient. This study investigated and compared the antimelanogenic effect of solvent-partitioned fractions of *C. japonicum* extract (CJEFs) in a B16F10 mouse melanoma cell model, focusing on tyrosinase activity and production. Melanogenesis is the process in which skin pigment melanin is produced through tyrosinase activity. Overproduction of melanin is the primary reason behind several skin disorders such as freckles, spots, and hyperpigmentation. The antimelanogenic capacity of CJEFs was initially screened by their tyrosinase inhibitory effects, prevention of dihydroxyphenylalanine (DOPA) oxidation, and suppression of melanin production. The inhibition of tyrosinase activity and DOPA oxidation by CJEFs was suggested to be related to the downregulation of microphthalmia-associated transcription factor, tyrosinase, tyrosinase-related protein-1, and tyrosinase-related protein-2, which was confirmed using mRNA and protein expression levels. Moreover, the glycogen synthase kinase 3 beta- and cyclic adenosine monophosphate response element-binding protein-related signaling pathways were inhibited by treatment with CJEFs, indicating their action mechanism. All the tested CJEFs exerted similar effects on tyrosinase activity and production. However, among those, 85% aq. MeOH was the most active fraction to suppress the signaling pathway that produces tyrosinase. These results suggest that especially the MeOH fraction of *C. japonicum* extract serves as a potential source of bioactive substances, with effective antimelanogenesis properties.

Keywords: *Cnidium japonicum*, dihydroxyphenylalanine, melanogenesis, tyrosinase, tyrosinase-related proteins

INTRODUCTION

The skin is always under attack from external factors during a lifetime, among which ultraviolet (UV) radiation is one of the most harmful factors and causes premature skin aging. The human skin has several cellular processes to counteract these harmful effects of environmental factors. The primary defense mechanism against UV-induced damages is skin pigmentation achieved through melanin synthesis (Nick, 2021). Exposure to UV radiation stimulates the production of melanin in skin cells to absorb the UV light and neutralize it. However, continuous exposure to UV radiation causes melanin accumulation in the skin as a result of overproduction (Ortonne and Bissett, 2008). This overproduction is the major effector of several skin pigmentation disorders such as age spots, discoloration, and freckles (Ortonne and Bissett, 2008; Vashi and Kundu, 2013). Several cosmeceuticals of both natural and synthetic origin have been developed to act against UV-induced melanin overproduction (Kanlayavattanakul and Lourith, 2018; Panzella and Napolitano, 2019).

Melanin synthesis, also known as melanogenesis, revolves around three critical proteins, viz., tyrosinase, tyrosinase-related protein (TRP)-1, and TRP-2. The activity and expression of these proteins are regulated by the activity of microphthalmia-associated transcription factor whose transcriptional activity is induced by upstream stimulation through the α-melanocyte-stimulating hor-

Received 5 October 2022; Revised 31 October 2022; Accepted 16 November 2022; Published online 31 December 2022

Correspondence to Chang-Suk Kong, E-mail: cskong@silla.ac.kr
Author information: Hyun Jin Jo (Graduate Student), Jung Hwan Oh (Professor), Fatih Karadeniz (Professor), Youngwan Seo (Professor), Chang-Suk Kong (Professor)

mone (α-MSH) (Nguyen and Fisher, 2019). Consequently, the expressed tyrosinase undergoes a maturation and activation process and initiates melanogenesis by hydroxylate L-tyrosine to yield L-3,4-dihydroxyphenylalanine (DOPA) that is subsequently converted into DOPA-quinone. Conversely, TRP-2 catalyzes the production of 5,6-dihydroxyindole-2-carboxylic acid (DHICA) from DOPA-chrome, and TRP-1 oxidizes DHICA to yield indole-5,6-quinone-2-carboxylic acid (Vachtenheim and Borovanský, 2010; Venkatesan et al., 2022). All these quinones are the precursors of melanin and used to produce brown/black-colored eumelanin or yellow/pink-colored pheomelanin.

Halophytes are salt marsh plants that can grow in extremely salty environments, primarily found in coastal seashores and salt dunes. The literature reports numerous potential bioactive compounds isolated from different species of halophytes, which exert diverse bioactivities ranging from antioxidant, antitumor, and antibacterial to antiaging, antiinflammatory, and antidiabetic activities (Arya et al., 2019; Giordano et al., 2021; Lopes et al., 2021). *Cnidium japonicum* Miq. is a common halophyte species found in the Western coasts of South Korea, habituating the muddy salt marshes along the ocean coastline. Although some preliminary research has indicated some potential bioactivities for *C. japonicum* (Yang et al., 2009; Shah et al., 2013), to the best of our knowledge, there has been no study evaluating its potential as an antimelanogenic cosmeceutical source. In this study, we used α-MSH-stimulated melanogenesis in a B16F10 mouse skin melanoma cell line as an *in vitro* model to investigate the effects of the fractions of *C. japonicum* extracts (CJEFs) on the overproduction of melanin.

MATERIALS AND METHODS

Plant material and extraction

C. japonicum collected from the coast of Donggeom-ri, Gilsang-myeon, Ganghwa-gun, Gyeonggi-do, was kindly provided by Korea Maritime and Ocean University (Busan, Korea). Whole plants were air-dried under shade and placed in methylene chloride (CH_2Cl_2) for 24 h at room temperature with occasional stirring. After 24 h, the supernatant was filtered and collected, and to the remaining residue, the same amount of CH_2Cl_2 was added and kept for another 24 h under the same conditions. After collecting the supernatant once more, the same procedure was conducted with MeOH as the solvent instead of CH_2Cl_2. Finally, the supernatants from each solvent extraction were mixed and dried using a rotary evaporator to obtain *C. japonicum* crude extract. Then, the crude extract was initially fractionated between CH_2Cl_2 and H_2O. The organic CH_2Cl_2 layer was then separated between *n*-hexane and 85% aq. MeOH, and the aqueous layer was fractionated between *n*-BuOH and H_2O to obtain different solvent fractions of CJEF. Subsequently, two compounds were isolated from the most active CJEF, 85% aq. MeOH, according to the present study results. Characterization of the chemical structures of the compounds columbianetin and libanoridin was conducted by comparing their structural data with published reports.

***Columbianetin*:** ^{1}H nuclear magnetic resonance (NMR) ($CDCl_3$, 900 MHz) δ 7.63 (^{1}H, d, J=9.5 Hz, H-4), 7.27 (^{1}H, d, J=8.3 Hz, H-5), 6.75 (^{1}H, d, J=8.3 Hz, H-6), 6.21 (^{1}H, d, 9.5 Hz, H-3), 4.80 (^{1}H, dd, J=9.5, 8.5 Hz, H-2′), 3.35 (^{1}H, dd, J=16.0, 9.5 Hz, H-1′), 3.30 (^{1}H, dd, 16.0, 8.5 Hz, H-1′), 1.83 (^{1}H, s, OH), 1.37 (^{3}H, s, H-4′/-5′), 1.24 (^{3}H, s, H-4′/-5′); ^{13}C NMR ($CDCl_3$, 225 MHz) δ 163.7 (C, C-7), 161.0 (C, C-2), 151.3 (C, C-9), 143.9 (CH, C-4), 128.7 (CH, C-5), 114.0 (C, C-10), 113.1 (C, C-8), 112.3 (CH, C-3), 106.7 (CH, C-6), 91.3 (CH, C-2′), 71.8 (C, C-3′), 27.6 (CH_2, C-1′), 26.0 (CH_3, C-4′/-5′), 23.9 (CH_3, C-4′/-5′)

***Libanoridin*:** ^{1}H NMR ($CDCl_3$, 900 MHz) δ 7.63 (^{1}H, d, J= 9.5 Hz, H-4), 7.27 (^{1}H, d, J=8.3 Hz, H-5), 6.75 (^{1}H, d, J= 8.3 Hz, H-6), 6.22 (^{1}H, d, J=9.5 Hz, H-3), 5.16 (^{1}H, dd, J=9.9, 7.7 Hz, H-2′), 3.38 (^{1}H, dd, J=16.2, 9.9 Hz, H-1′), 3.34 (^{1}H, dd, J=16.2, 7.7 Hz, H-1′), 1.99 (^{3}H, s, H-7′), 1.57 (^{3}H, s, H-4′/-5′), 1.52 (^{3}H, s, H-4′/-5′); ^{13}C NMR (75 MHz, $CDCl_3$) δ: 170.3 (C, C-6′), 163.9 (C, C-7), 161.0 (C, C-2), 151.3 (C, C-9), 144.0 (CH, C-4), 128.8 (CH, C-5), 113.4 (C, C-10), 113.1 (C, C-8), 112.2 (CH, C-3), 106.7 (CH, C-6), 88.7 (CH, C-2′), 82.1 (C, C-3′), 27.6 (CH_2, C-1′), 22.2 (CH3, C-7′), 22.0 (CH_3, C-4′/-5′), 20.9 (CH_3, C-4′/-5′).

Mushroom tyrosinase activity inhibition

The antimelanogenic effects of CJEFs were first tested on the activity of tyrosinase enzyme using a mushroom tyrosinase assay model. Briefly, 110 μL of 0.1 M phosphate buffer saline (PBS, pH 6.5) containing 10 μL of CJEFs at varying concentrations (10, 20, 30, 40, and 50 μg/mL) was added to the wells of a 96-well transparent plate. Then, 10 μL of mushroom tyrosinase (1,800 U/mL) enzyme solution was added to each well, and the oxidation reaction was initiated by the addition of 20 μL of L-tyrosine (1.5 mM), the substrate of tyrosinase. The reaction was performed at 37°C for 15 min, after which the oxidation of L-tyrosine by tyrosinase in the presence of CJEFs was measured using the absorbance values of each well at 490 nm using the Infinite F200 microplate reader (Tecan Austria GmbH, Männedorf, Switzerland). The antimelanogenic compound Kojic acid (1 μM) was used as a positive control.

Inhibition of L-DOPA oxidation

Following the inhibition of tyrosinase activity, the ability of CJEFs to obstruct the subsequent steps of melanogen-

esis was evaluated by their inhibitory effect on L-DOPA oxidation by tyrosinase. Briefly, 170 μL of PBS (pH 7.0) containing 10 μL of CJEFs at varying concentrations (10, 20, 30, 40, and 50 μg/mL) was added to each well of a transparent 96-well plate. Then, 10 μL of mushroom tyrosinase (1,800 U/mL) enzyme solution was added to each well, and the oxidation reaction was initiated by the addition of 10 μL of L-DOPA (10 mM), the substrate of tyrosinase. The plate was then kept at 37°C for 10 min, after which the absorbance values were measured at 475 nm using the Tecan Infinite F200 microplate reader (Tecan Austria GmbH) to quantify the L-DOPA oxidation into dopaquinone. As a positive control, the antimelanogenic compound Kojic acid (1 μM) was used.

Cell culture, maintenance, and melanogenesis stimulation

Cellular assays were conducted to evaluate the antimelanogenic effects of CJEFs in B16F10 murine melanoma cells that were purchased from Korea Cell Line Bank (Seoul, Korea). To mimic UV-induced overproduction of melanin, cells were stimulated with 100 nM α-MSH. A separate blank group was also cultured as a negative control without α-MSH stimulation and CJEF treatment. The cells were propagated in T-25 cell culture flasks before seeding into 96- or 6-well plates for assays. The cells were fed with Dulbecco's modified Eagle's medium (Welgene, Gyeongsan, Korea) containing 10% fetal bovine serum (Welgene) and 1% L-glutamine penicillin-streptomycin solution (Welgene). Between experiments, the cells were placed in incubators at 37°C and 5% CO_2.

Cytotoxicity of CJEFs

Before conducting investigations on the antimelanogenic effects, any cytotoxic presence of CJEFs in B16F10 melanoma cells was confirmed using a common 3-(4,5-dimethylthiazol-2-yl)-2,5-diphenyltetrazolium bromide (MTT) assay. Briefly, cells were seeded in 96-well plates at a density of 3×10^3 cells per well and incubated for 24 h. After incubation, the cells were treated with increasing concentrations of CJEFs for an additional 24 h. Next, the wells were aspirated and filled with 100 μL of MTT reagent (0.05%, m/v) and incubated for another 4 h. The viability of the cells was measured by the ability of alive cells to turn MTT into purple formazan crystals. The reaction was stopped by adding 100% dimethyl sulfoxide (DMSO) to each well after 4 h of incubation, and the viability levels were quantified as a relative percentage of the untreated control measured using absorbance values at 540 nm obtained using the Tecan Infinite F200 microplate reader (Tecan Austria GmbH).

Inhibition of cellular tyrosinase production

The tyrosinase production levels of CJEF-treated B16F10 cells were examined by the ability of L-DOPA oxidation of cell lysates. Briefly, cells were plated in 6-well plates at a density of 5×10^4 cells per well and incubated for 24 h before CJEF treatment. Melanogenesis was stimulated in the cells using α-MSH (100 nM) alone or combined with 1, 5, and 25 μg/mL of CJEFs. At the end of the treatment, the wells were aspirated and washed with PBS. Subsequently, the cells were lysed by vigorous agitation and the addition of 200 μL of lysis buffer (5 mM EDTA, 0.1 M sodium phosphate buffer, pH 6.8, 1% Triton X-100, and 0.1 mM phenylmethylsulfonyl fluoride). Cell lysates were then transferred into microcentrifuge tubes and centrifuged at 1,000 *g* for 5 min. Supernatants were harvested and used for tyrosinase activity assay after the quantification of total protein using Bio-Rad protein assay solution (Bio-Rad Laboratories, Hercules, CA, USA). The assay mixtures in the tubes contained the cell lysate containing same amount of protein and 0.1 M sodium phosphate buffer (pH 6.8) at a ratio of 1:3. Oxidation was initiated by adding 50 μL of the tyrosinase substrate L-DOPA (0.1% w/v) to the assay mixture. Tubes were placed at 37°C for 1 h, after which the absorbance values were recorded at 490 nm using a microplate reader (Tecan Austria GmbH). Tyrosinase activity was quantified as a relative absorbance value compared with the α-MSH-stimulated untreated control group.

Inhibition of intracellular melanin content and melanin secretion

The intracellular melanin content of B16F10 murine melanoma cells following α-MSH stimulation in the presence or absence of CJEFs was measured using the cell lysates obtained in the intracellular tyrosinase production assay. Cell lysates were washed with ice-cold 75% EtOH and left at room temperature for drying. Dried lysates were suspended in 200 μL of 1 N NaOH containing 1% DMSO. The melanin in the lysates was dissolved by heating the suspended lysates at 80~90°C for 1 h. Finally, the melanin content of the lysates was quantified by plotting the absorbance value of 50 μL of the lysate at 405 nm against a standard curve. A standard calibration curve was plotted using purified melanin (Sigma-Aldrich Co., St. Louis, MO, USA) and measuring the absorbance of different purified melanin concentrations at 405 nm.

The inhibition of melanin secretion by CJEF treatment was evaluated in α-MSH-stimulated B16F10 murine melanoma cells. Melanogenesis stimulation and sample treatment of the cells were performed in the same manner as mentioned in the cellular tyrosinase production inhibition assay. After the completion of the treatment, the cell culture medium from each well was harvested and used for the detection of melanin levels. Briefly, 50 μL of culture medium was transferred into the wells of a 96-well plate, and the absorbance values were measured at 405 nm. The melanin content was quantified using a standard curve

plotted using the absorbance values of melanin samples compared with known concentrations.

Inhibition of mRNA and protein expression of melanogenesis-related proteins

The mRNA expression levels of melanogenesis-related proteins were analyzed using a common reverse transcriptase-polymerase chain reaction analysis. Treatment and incubation of the cells were performed as mentioned earlier (Lee et al., 2017). At the end of the treatment, total RNA was isolated from the cells using Trizol reagent (Invitrogen Co., Carlsbad, CA, USA) and vigorous pipetting. Subsequent steps of cDNA synthesis and target gene multiplication were performed as described earlier using the specific primers shown in Table 1.

The content of melanogenesis-related proteins in the total protein of B16F10 cells was evaluated by traditional western blotting. Briefly, cells treated and incubated as described earlier were subjected to total protein isolation using the radio-immunoprecipitation assay lysis buffer for 30 min at 4°C. The total protein amount in the cell lysates was quantified using Bio-Rad protein assay according to the manufacturer's instructions (Bio-Rad Laboratories). Similar amounts of protein from each treatment group were separated by 12% sodium dodecyl sulfate-polyacrylamide gel electrophoresis. The separated proteins were then transferred onto polyvinylidene fluoride membranes (Amersham Pharmacia Biotech., Amersham, UK) using a prepacked wet transfer system, Trans-Blot Turbo Transfer System (Bio-Rad Laboratories). The specific primary antibodies used for the detection of melanogenesis-related proteins are mentioned in a previous study (Lee et al., 2017). The specific protein bands were then visualized following incubation with horseradish-peroxidase-conjugated secondary antibody at room temperature and using a commercial chemiluminescence enhanced chemiluminescence assay kit (Amersham Pharmacia Biosciences). Images of the bands were taken using Davinch-Chemi CAS-400SM Imager (Davinch-K, Seoul, Korea).

Table 1. Gene-specific primers used for real time-PCR

Gene	Sequence (5′→3′)
MITF	
Forward	AAC-CGA-CAG-AAG-AAG-CTG-GA
Reverse	ACA-AGT-TCC-TGG-CTG-CAC-TT
Tyrosinase	
Forward	TTA-TGC-GAT-GGA-ACA-CCT-GA
Reverse	ACT-GGC-AAA-TCC-TTC-CAG-TG
TRP-1	
Forward	AGG-AAT-CTG-GCT-TGG-GAT-TT
Reverse	AGA-AGA-CAG-GGG-TGC-TCA-GA
TRP-2	
Forward	AGC-AGA-CGG-AAC-ACT-GGA-CT
Reverse	GCA-TCT-GTG-GAA-GGG-TTG-TT
β-Actin	
Forward	CCA-CAG-CTG-AGA-GGG-AAA-TC
Reverse	AAG-GAA-GGC-TGG-AAA-AGA-GC

MITF, microphthalmia-associated transcription factor; TRP, tyrosinase-related protein.

Statistical analysis

Data were expressed as mean±standard deviation (n=3) wherever applicable. Significant differences between the mean values of the different treatment groups were expressed at the $P<0.05$ level calculated by one-way analysis of variance coupled with Duncan's multiple range post hoc test (SAS v9.1, SAS Institute, Cary, NC, USA).

RESULTS AND DISCUSSION

Effect of CJEFs on tyrosinase activity

Before conducting cell-based assays to evaluate the antimelanogenic potential of CJEFs, their tyrosinase inhibitory properties were tested on mushroom tyrosinase using L-tyrosine and L-DOPA as substrates. All the tested CJEFs exerted remarkable inhibitory effects on the activity of tyrosinase on L-tyrosine, the initial step of melanin production (Table 2). Among the CJEFs, 85% aq. MeOH was the most active fraction with an half maximal inhibitory concentration (IC_{50}) value of 139.3 μg/mL, followed by *n*-hexane with an IC_{50} value of 153.2 μg/mL, whereas H_2O and *n*-BuOH were the least active fractions with IC_{50} values of 237.1 and 237.2 μg/mL, respectively. A similar inhibition trend was observed on L-DOPA oxidation by mushroom tyrosinase (Fig. 1). At the highest dose (50 μg/mL), 85% aq. MeOH CJEF inhibited L-DOPA oxidation by 30.9% of that of the untreated control group. The inhibition rates for *n*-hexane, H_2O, and *n*-BuOH CJEFs were 28.2%, 21%, and 20.4%, respectively. Although the inhibitory activities of CJEFs were not comparable to that of Kojic acid, they potentially contained inhibitory constituents.

Effect of CJEFs on tyrosinase activity and production in B16F10 cells

We next used B16F10 murine melanoma cells to explore the effects of the fractions on melanogenesis. Melanin production in B16F10 cells is generally not significant to

Table 2. The IC_{50} values of different solvent fractionated *Cnidium japonicum* extracts on the *in vitro* mushroom tyrosinase activity (unit: μg/mL)

Solvent	IC_{50} value
H_2O	237.1
n-BuOH	237.2
85% aq. MeOH	139.3
n-Hexane	153.2

IC_{50}, the half maximal inhibitory concentration.

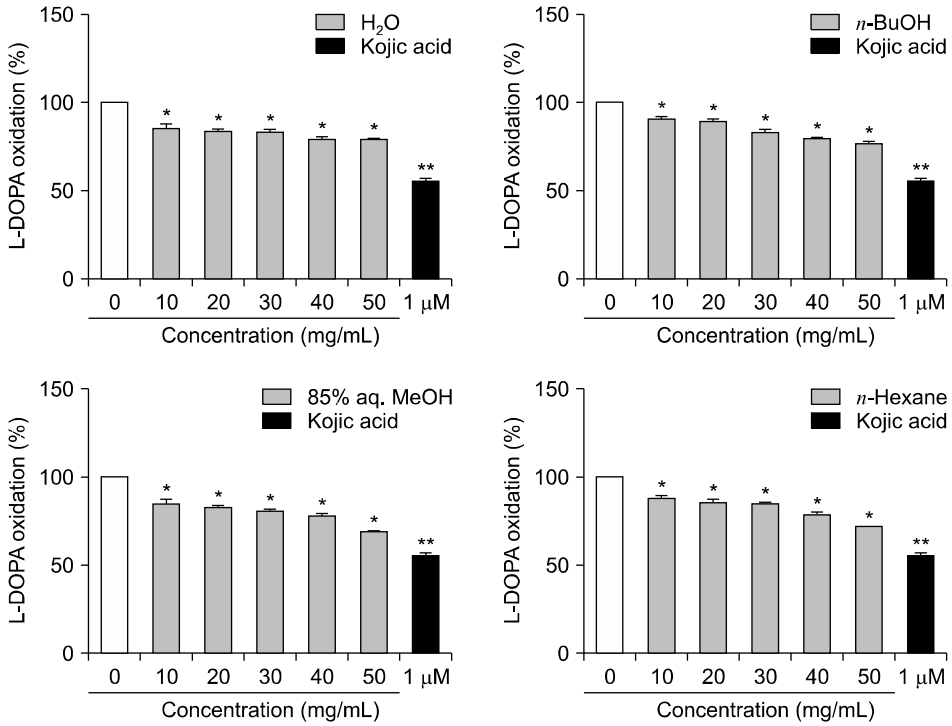

Fig. 1. Effect of *Cnidium japonicum* extracts on the *in vitro* L-3,4-dihydroxyphenylalanine (L-DOPA) oxidation of mushroom tyrosinase. Inhibition of L-DOPA oxidation is represented as a relative percentage of untreated α-melanocyte-stimulating hormone-stimulated control group. Kojic acid, a tyrosinase inhibitor, was used as a positive control. An unstimulated untreated cell group was used as a negative control. **P*<0.05 and ***P*<0.01 vs. untreated group.

detect antimelanogenic activities. Therefore, cells were stimulated with α-MSH, a common melanogenesis inducer used in similar studies. The induction of melanin production by α-MSH follows the same signaling downstream with the UV-induced increase in melanin production (Videira et al., 2013; Chen et al., 2021). Therefore, α-MSH-stimulated melanoma cells were established to act as a UV-induced melanogenic production model to evaluate the antimelanogenic potential of CJEFs. However, before any assay using the cells, the cytotoxicity of the CJEFs was examined to detect any antimelanogenic effect as a bioactivity of CJEF ingredients rather than a toxic presence. Cell viability assays revealed that the CJEF treatment exerted no significant toxicity in B16F10 cells at up to 25 μg/mL concentration (Fig. 2A). Therefore, this concentration was chosen as the upper limit for further CJEF treatment.

First, the tyrosinase levels in CJEF-treated cells were analyzed by measuring the tyrosinase activity of treated and untreated groups. As shown in Fig. 2B, all CJEFs induced a dose-dependent decrease in tyrosinase activity, which was strongly increased in the untreated α-MSH-stimulated group compared to that in the unstimulated untreated control group. The decrease in tyrosinase activity was 45.2% of that in the untreated group in cells treated with 25 μg/mL of 85% aq. MeOH CJEF. Treat-

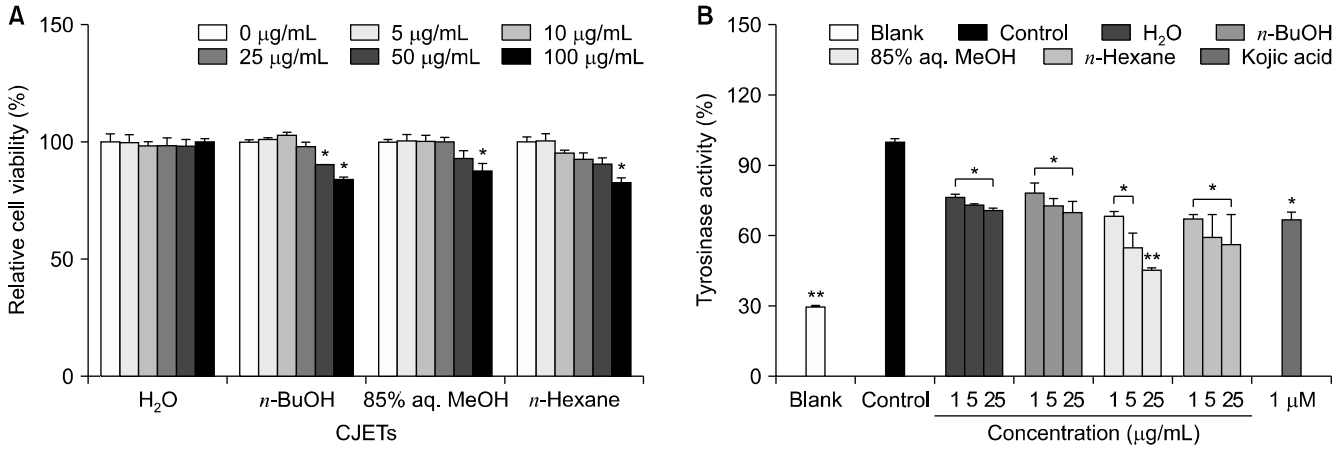

Fig. 2. Effect of *Cnidium japonicum* extracts (CJEFs) on cell viability (A) and total active tyrosinase levels (B) in B16F10 murine melanoma cells. Active tyrosinase levels were measured by their ability to oxidize L-3,4-dihydroxyphenylalanine. Intracellular tyrosinase activity is expressed as a relative percentage of untreated α-melanocyte-stimulating hormone (α-MSH)-stimulated control group (Control). Kojic acid, a tyrosinase inhibitor, was used as a positive control. An unstimulated untreated cell group was used as a negative control (Blank). **P*<0.05 and ***P*<0.01 vs. untreated group (A) and vs. α-MSH-stimulated untreated group (B).

ment with *n*-hexane CJEF decreased the tyrosinase activity to 56.1% of that in the untreated group, whereas treatment with H_2O and *n*-BuOH CJEFs resulted in 29.3% and 30.1% decreases, respectively. These results were consistent with mushroom tyrosinase inhibitory activities of CJEFs, as the most active CJEF was 85% aq. MeOH. The results also indicated that in addition to inhibiting the activity of tyrosinase, 85% aq. MeOH could decrease the total intracellular active tyrosinase levels.

Effect of CJEFs on melanin production in B16F10 cells

Next, we evaluated both the intracellular and secreted melanin content of α-MSH-stimulated and nonstimulated cells to confirm whether the effect of CJEFs on tyrosinase activity and production translated into diminished melanin production. As shown in Fig. 3, α-MSH stimulation significantly elevated the production of melanin. Treatment with all CJEFs resulted in a remarkable dose-dependent decrease in both secreted (Fig. 3A) and intracellular (Fig. 3B) melanin levels starting from the lowest dose of 1 μg/mL. Similar to previous results, treatment with 85% aq. MeOH CJEF resulted in the highest decrease of extracellular melanin content. However, treatment with *n*-hexane CJEF resulted in the maximum decrease of intracellular melanin levels compared with other CJEFs. These results indicated that the effect of CJEFs on tyrosinase activity led to a consequent decrease in melanin production, exerting a pigmentation-hindering effect. Considering the overall results, 85% aq. MeOH was the most active CJEF with more potential to contain antimelanogenic substances that may inhibit tyrosinase activity and/or tyrosinase expression. Some studies have indicated that antioxidant natural products exhibit pigmentation-delaying properties by scavenging oxygen and nitrogen species as well as reducing intermediate quinone derivatives that play roles in the oxidative polymerization steps of melanogenesis (Nahhas et al., 2019; Xing et al., 2022). In this context, halophytes are known for their diverse and abundant content of antioxidants (Surówka and Hura, 2020). Moreover, UV radiation was suggested to increase the α-MSH-mediated tyrosinase production using free radicals whose levels were elevated during prolonged exposure to UV (Nahhas et al., 2019). It can be postulated that the 85% aq. MeOH CJEF consisted of the highest number of substances with antioxidant properties that could prevent UV-induced overpigmentation in melanocytes.

Therefore, the effect of CJEFs on the signaling pathway of melanogenesis activation was investigated by examining the expression of related proteins. The 85% aq. MeOH fraction was the most active CJEF when all the results were considered. Therefore, it was subjected to further mRNA and protein expression analyses to confirm its activity on the intracellular signaling cascades that regulate melanin synthesis. First, the mRNA and protein expression levels of melanogenesis-progressing proteins, tyrosinase, TRP-1, and TRP-2 were observed under treatment with 85% aq. MeOH CJEF. B16F10 cells were exposed to α-MSH (100 nM) in the presence or absence of CJEF (1, 5, and 25 μg/mL), and mRNA levels were examined by real time-PCR. All treated cells exhibited decreased mRNA levels for tyrosinase, TRP-1, and TRP-2 (Fig. 4A). These results were also further confirmed by the similar suppression trend in tyrosinase protein levels analyzed by western blotting (Fig. 4B). Treatment with 85% aq. MeOH CJEF resulted in the suppression of tyrosinase activity in a concentration-dependent manner, which might the reason for the CJEF-induced decrease of α-MSH-mediated elevation of melanogenesis.

Other *Cnidium* species have also been reported in the context of melanogenesis. For instance, Cha (2018) reported that extracts obtained from *Cnidium officinale* Makino inhibited α-MSH-induced melanogenesis in B16F10 mouse melanoma cells. Results showed that *C. officinale*

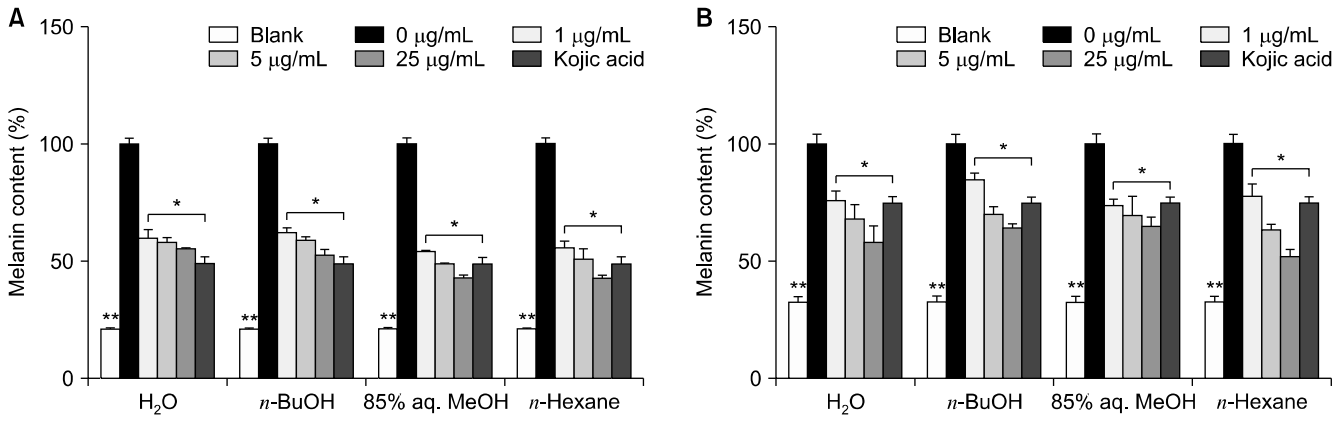

Fig. 3. Effect of *Cnidium japonicum* extracts on the extracellular (A) and intracellular (B) melanin content in α-melanocyte-stimulating hormone (α-MSH)-stimulated B16F10 murine melanoma cells. Melanin content is represented as a relative percentage of untreated α-MSH-stimulated control group. Kojic acid, a tyrosinase inhibitor, was used as a positive control. An unstimulated untreated cell group was used as a negative control (Blank). $^*P<0.05$ and $^{**}P<0.01$ vs. α-MSH-stimulated untreated group.

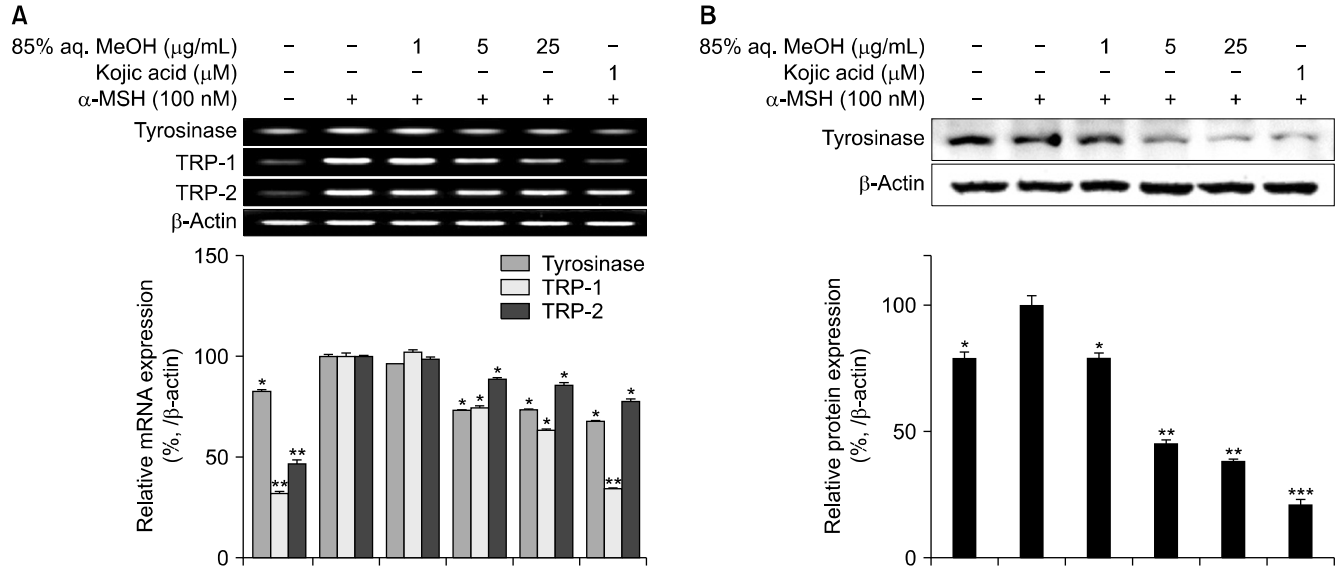

Fig. 4. Effect of 85% aq. MeOH *Cnidium japonicum* extract on the mRNA expression of melanogenesis-related factors, tyrosinase, tyrosinase-related protein (TRP)-1, and TRP-2 (A) and protein expression of tyrosinase (B) in α-melanocyte-stimulating hormone (α-MSH)-stimulated B16F10 murine melanoma cells analyzed by real time-PCR and western blotting, respectively. Bands were densiometrically quantified, normalized against internal loading control β-actin, and represented as the relative percentage of α-MSH-stimulated untreated control group. An unstimulated untreated cell group was used as a negative control. $^{*}P<0.05$, $^{**}P<0.01$, and $^{**}P<0.001$ vs. α-MSH-stimulated untreated group.

extracts exerted similar effects as those of CJEFs on tyrosinase expression and melanin production. Furthermore, Um et al. (2017) reported that fermented extracts of *C. officinale* exerted antioxidant, antiwrinkle, and whitening effects in B16F10 cells. In another study by Kim et al. (2016), *Cnidium monnieri* fruits yielded a bioactive coumarin osthol, which is a potent melanogenesis inhibitor. Optimization for the extraction of osthol was also performed by analyzing the expression levels of TRP-1 and TRP-1. Similarly, the bioactive ingredients from CJEFs are expected to possess antimelanogenic properties. It was suggested that the coumarin constituents of CJEFs would exert similar antimelanogenic effects.

Isolation of columbianetin and libanoridin and their effect on melanin production

After confirming the activity of 85% aq. MeOH CJEF on α-MSH-induced melanogenesis, it was subjected to further isolation by high-performance liquid chromatography (Fig. 5A), which yielded two known compounds, columbianetin and libanoridin (Fig. 5B), both of which are bioactive compounds with reported bioactivities (Ahn et al., 2013; Oh and Hyun, 2022). These compounds and others with similar chemical structures might be the active constituents of CJEFs that exhibited antimelanogenic properties. To confirm this assumption, their effect on melanin production in α-MSH-stimulated B16F10 cells was evaluated. As anticipated, both compounds resulted in a dose-dependent decrease in α-MSH-mediated melanin production (Fig. 5C).

In conclusion, *C. japonicum* might contain antimelanogenic secondary metabolites that can be used against hyperpigmentation. Specifically, the 85% aq. MeOH fraction of *C. japonicum* crude extract, which yielded the two potential antimelanogenic compounds columbianetin and libanoridin, was proposed to be abundant in such substances and warrant further investigations to isolate and characterize novel cosmeceuticals for protection against UV-induced pigmentation problems. Moreover, some studies have reported the possible antitumor properties of coumarins and their derivatives from *Cnidium* species, which provides further significance to the isolation of novel compounds from CJEFs (Sumiyoshi et al., 2014; Duan et al., 2019). In addition, there is a lack of research in the literature on the antimelanogenic properties of columbianetin and libanoridin. The present study suggested that the 85% aq. MeOH CJEF and its constituents exhibited strong antimelanogenic potential. However, further investigations using *in vivo* and 3D skin models are required to establish the antimelanogenic properties of columbianetin and libanoridin and even other constituents that might be isolated. Nonetheless, the 85% aq. MeOH fraction from *C. japonicum* might contain strong antimelanogenic compounds such as columbianetin and libanoridin, and further studies to utilize *C. japonicum*-sourced cosmeceuticals are recommended.

FUNDING

This research was supported by the BB21plus funded by Busan Metropolitan City and Busan Institute for Talent

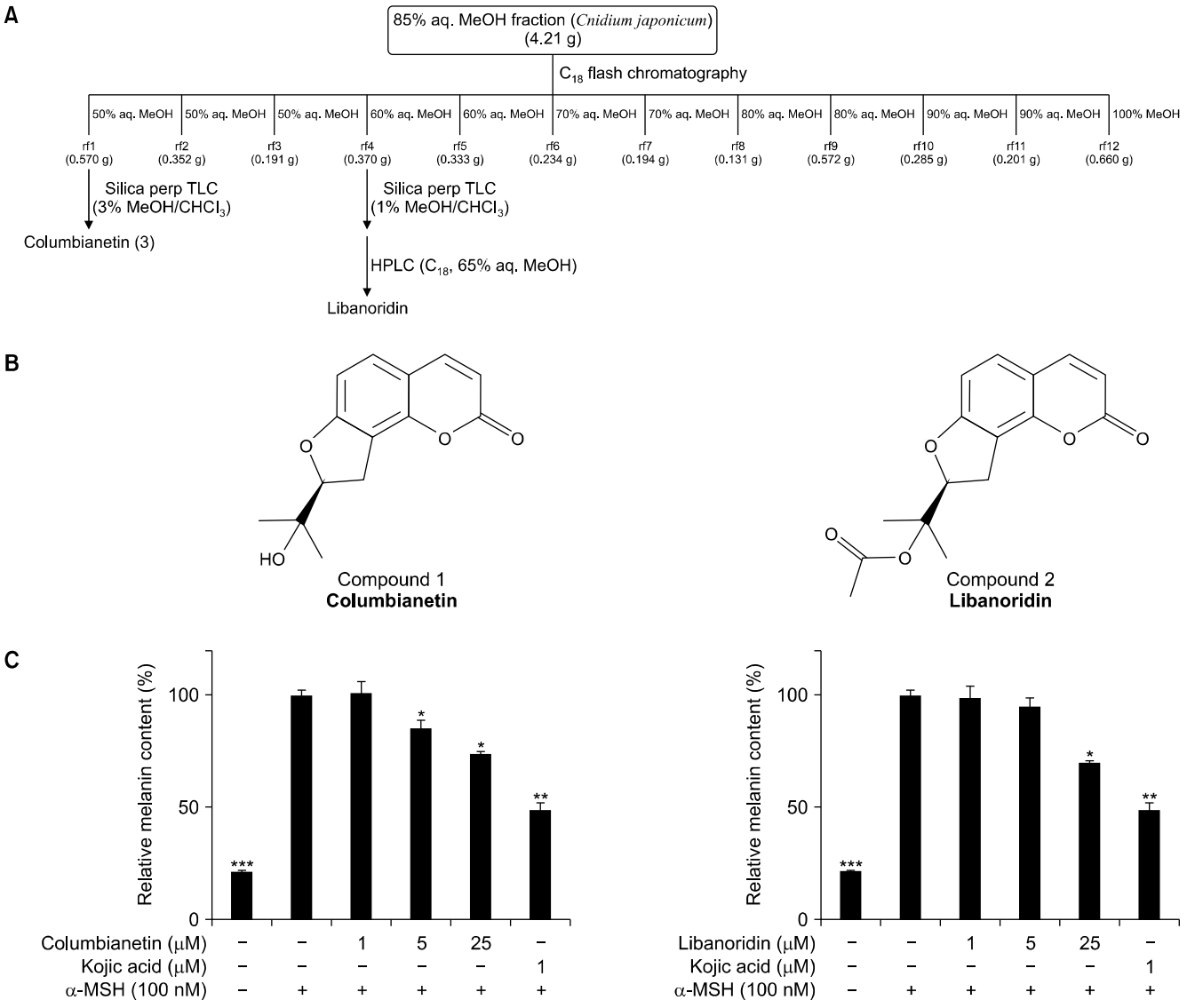

Fig. 5. Isolation scheme (A) and the chemical structures (B) of the active compounds columbianetin and libanoridin and their effect on melanin content in α-melanocyte-stimulating hormone (α-MSH)-stimulated B16F10 murine melanoma cells (C). Melanin content is expressed as a relative percentage of untreated α-MSH-stimulated control group. Kojic acid, a tyrosinase inhibitor, was used as a positive control. An unstimulated untreated cell group was used as a negative control. **P*<0.05, ***P*<0.01, and ***P*<0.001 vs. α-MSH-stimulated untreated group. TLC, thin layer chromatography; HPLC, high-performance liquid chromatography.

& Lifelong Education (BIT) and the Korea Institute of Marine Science and Technology Promotion (KIMST) and funded by the Ministry of Oceans and Fisheries, Korea (no. 20220259).

AUTHOR DISCLOSURE STATEMENT

The authors declare no conflict of interest.

AUTHOR CONTRIBUTIONS

Concept and design: HJJ, JHO, CSK. Analysis and interpretation: JHO, FK, YS. Data collection: HJJ, JHO, FK. Writing the article: JHO, FK. Final approval of the article: all authors. Statistical analysis: FK, YS. Obtained funding: CSK. Overall responsibility: CSK.

REFERENCES

Ahn BN, Kim JA, Kong CS, Seo Y, Kim SK. Photoprotective effect of libanoridin isolated from *Corydalis heterocarpa* on UVB stressed human keratinocyte cells. Exp Dermatol. 2013. 22:155-157.

Arya SS, Devi S, Ram K, Kumar S, Kumar N, Mann A, et al. Halophytes: the plants of therapeutic medicine. In: Hasanuzzaman M, Nahar K, Öztürk M, editors. Ecophysiology, Abiotic Stress Responses and Utilization of Halophytes. Springer, Singapore, Singapore. 2019. p 271-287.

Cha HJ. *Cnidium officinale* Makino extracts inhibit α-MSH-induced melanogenesis in B16F10 mouse melanoma cells. Asian J Beauty Cosmetol. 2018. 16:122-130.

Chen J, Liu Y, Zhao Z, Qiu J. Oxidative stress in the skin: Impact

and related protection. Int J Cosmet Sci. 2021. 43:495-509.
Duan YD, Jiang YY, Guo FX, Chen LX, Xu LL, Zhang W, et al. The antitumor activity of naturally occurring chromones: A review. Fitoterapia. 2019. 135:114-129.
Giordano R, Saii Z, Fredsgaard M, Hulkko LSS, Poulsen TBG, Thomsen ME, et al. Pharmacological insights into halophyte bioactive extract action on anti-inflammatory, pain relief and antibiotics-type mechanisms. Molecules. 2021. 26:3140. https://doi.org/10.3390/molecules26113140
Kanlayavattanakul M, Lourith N. Plants and natural products for the treatment of skin hyperpigmentation—a review. Planta Med. 2018. 84:988-1006.
Kim SB, Kim C, Liu Q, Jo YH, Choi HJ, Hwang BY, et al. Optimization of extraction conditions for osthol, a melanogenesis inhibitor from *Cnidium monnieri* fruits. Pharm Biol. 2016. 54:1373-1379.
Lee SG, Karadeniz F, Seo Y, Kong CS. Anti-melanogenic effects of flavonoid glycosides from *Limonium tetragonum* (Thunb.) bullock via inhibition of tyrosinase and tyrosinase-related proteins. Molecules. 2017. 22:1480. https://doi.org/10.3390/molecules22091480
Lopes M, Sanches-Silva A, Castilho M, Cavaleiro C, Ramos F. Halophytes as source of bioactive phenolic compounds and their potential applications. Crit Rev Food Sci Nutr. 2021. https://doi.org/10.1080/10408398.2021.1959295
Nahhas AF, Abdel-Malek ZA, Kohli I, Braunberger TL, Lim HW, Hamzavi IH. The potential role of antioxidants in mitigating skin hyperpigmentation resulting from ultraviolet and visible light-induced oxidative stress. Photodermatol Photoimmunol Photomed. 2019. 35:420-428.
Nguyen NT, Fisher DE. MITF and UV responses in skin: From pigmentation to addiction. Pigment Cell Melanoma Res. 2019. 32:224-236.
Nick P. Black is beautiful (and protective): melanin synthesis in animals and plants. Protoplasma. 2021. 258:923-924.
Oh SY, Hyun CG. Chrysoeriol enhances melanogenesis in B16F10 cells through the modulation of the MAPK, AKT, PKA, and Wnt/β-catenin signaling pathways. Nat Prod Commun. 2022. https://doi.org/10.1177/1934578X211069204
Ortonne JP, Bissett DL. Latest insights into skin hyperpigmentation. J Investig Dermatol Symp Proc. 2008. 13:10-14.
Panzella L, Napolitano A. Natural and bioinspired phenolic compounds as tyrosinase inhibitors for the treatment of skin hyperpigmentation: recent advances. Cosmetics. 2019. 6:57. https://doi.org/10.3390/cosmetics6040057.
Shah A, Varma C, Patankar S, Kadam V. Plant glycosides and aglycones displaying antiproliferative and antitumour activities—a review. Curr Bioact Compd. 2013. 9:288-305.
Sumiyoshi M, Sakanaka M, Taniguchi M, Baba K, Kimura Y. Antitumor effects of various furocoumarins isolated from the roots, seeds and fruits of *Angelica* and *Cnidium* species under ultraviolet A irradiation. J Nat Med. 2014. 68:83-94.
Surówka E, Hura T. Osmoprotectants and nonenzymatic antioxidants in halophytes. In: Grigore MN, editor. Handbook of Halophytes: From Molecules to Ecosystems towards Biosaline Agriculture. Springer, Cham, Switzerland. 2020. p 1901-1930.
Um JN, Min JW, Joo KS, Kang HC. Antioxidant, anti-wrinkle activity and whitening effect of fermented mixture extracts of *Angelica gigas*, *Paeonia Lactiflora*, *Rehmannia chinensis* and *Cnidium officinale*. Korean J Med Crop Sci. 2017. 25:152-159.
Vachtenheim J, Borovanský J. "Transcription physiology" of pigment formation in melanocytes: central role of MITF. Exp Dermatol. 2010. 19:617-627.
Vashi NA, Kundu RV. Facial hyperpigmentation: causes and treatment. Br J Dermatol. 2013. 169:41-56.
Venkatesan H, Soundhararajan R, Srinivasan H. Interaction of various types of bisphenols with enzymes involved in melanin synthesis. Toxicol Environ Health Sci. 2022. 14:19-24.
Videira IF, Moura DF, Magina S. Mechanisms regulating melanogenesis. An Bras Dermatol. 2013. 88:76-83.
Xing X, Dan Y, Xu Z, Xiang L. Implications of oxidative stress in the pathogenesis and treatment of hyperpigmentation disorders. Oxid Med Cell Longev. 2022. 2022:7881717. https://doi.org/10.1155/2022/7881717
Yang EJ, Yim EY, Song G, Kim GO, Hyun CG. Inhibition of nitric oxide production in lipopolysaccharide-activated RAW 264.7 macrophages by Jeju plant extracts. Interdiscip Toxicol. 2009. 2:245-249.